A boundary-element-based optimization technique for design of enclosure acoustical treatments

T. C. Yang
Center for Measurement Standards, Industrial Technology Research Institute, 321 Sec. 2, Kuang Fu Road, Hsinchu 30042, Taiwan, Republic of China

C. H. Tseng
Department of Mechanical Engineering, National Chiao Tung University, 1001 Ta Hsueh Road, Hsinchu 30050, Taiwan, Republic of China

S. F. Ling
School of Mechanical and Production Engineering, Nanyang Technological University, Nanyang Avenue, Singapore 2263, Singapore

(Received 7 September 1994; revised 31 January 1995; accepted 16 February 1995)

An effective design tool was developed in this study for solving the acoustical treatments in enclosures at low frequencies. The boundary element method was used for accurately predicting sound fields of an acoustical system. The sequential quadratic programming was selected as the continuous design variable optimizer as a result of its robustness and rapid convergence. In coping with the noncontinuous design variables, the optimizer was enhanced by a modified branch and bound procedure. A small two-dimensional cavity and an irregularly shaped car cabin were applied to demonstrate the utilities of the proposed design tool. Computer simulations indicated that at a low frequency, where enclosures can properly be termed as tightly coupled, purely reactive acoustical treatments are generally preferred at resonances or near-resonances of the two-dimensional cavity as well as at the frequency of interest in the car cabin. The general agreement between this study and previous work [R. J. Bernhard and S. Takeo, J. Acoust. Soc. Am. **83**, 2224–2232 (1988)] could be considered adequate for the proposed tool to be utilized for preliminary design studies of acoustical treatments in enclosures. Furthermore, in the case of multiple patching, the optimal locations of acoustical treatments would always contain the region of dominantly acoustical influence. However, simultaneous capability of optimizing locations and impedances of acoustical material were not considered in the previous work.

PACS numbers: 43.50.Gf, 43.55.Ka, 43.55Dt

INTRODUCTION

The design of effective noise control treatments for enclosures where typical dimensions are comparable with acoustic wavelengths, and/or sound sources and enclosures are geometrically complex, is relatively difficult. Such acoustical cavity systems are complicated by the near-field source effects, standing wave characteristics, and low-frequency behavior of typical sound treatments. The passenger compartments of a car and a propeller-driven aircraft, and enclosures of close-fitting appliances and business machine enclosures are such important applications where either the noise source is of low frequency or the enclosure is quite small. However, effective design procedures for such applications are rarely due to the complexity of the problems. Therefore, a reliable modeling procedure capable of accurately predicting the acoustical behaviors in enclosures as well as providing the design optimization information is fundamentally necessary.

Absorption of the low-frequency components of unwanted noise in cavities is difficult and expensive by conventional methods of using porous materials because of the thickness required. Through the extensive investigations of Maa[1,2] and Lee and Swenson,[3] however, noise control for low frequencies by passive techniques has become practical. Thus the possibility of employing passive techniques to effectively control low-frequency sound radiated from somewhere inside the cavity appears worthy of investigation.

Previous studies on the modeling techniques were useful for enclosures where either high-frequency statistical behavior can be assumed or the geometrical configuration is relatively simple.[4–7] In this study, simulation results obtained by optimally placing acoustical materials on the boundary of enclosures are provided to achieve a better noise control. The boundary element method (BEM), emerging as a powerful alternative to the finite element method (FEM) and only discretizing the surface rather than the volume, is chosen as an analysis tool for evaluating the acoustical characteristics in enclosed spaces. An optimizer employing the sequential quadratic programming (SQP) algorithm[8] is integrated with the boundary element acoustical analysis for accurately solving the aforementioned acoustical treatment problems in cavities.

Locating the proper positions of the sound absorbing materials on the boundary of enclosures is nearly impossible without the assistance of optimization techniques. In previous work, e.g., Bernhard and Takeo,[7] only the acoustical impedances of absorbing materials in a fixed position were optimized; in addition, all of the design variables were considered as the continuous type. However, both the acous-

 0001-4966/95/98(1)/302/11/$6.00

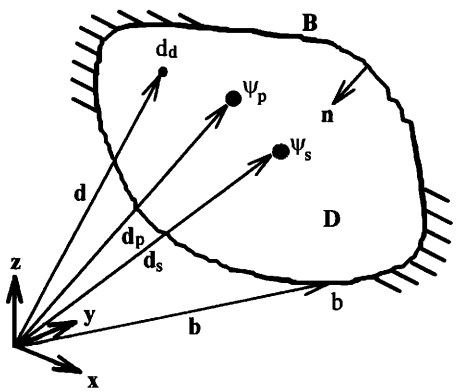

FIG. 1. Domain of acoustic system utilized for interior Helmholtz wave equation.

tical impedance and location of the absorbing material are simultaneously determined in this study for making the potential technique useful. Constraints, i.e., geometrical and/or functional, are also included as required due to practical considerations. From practical and economic concerns, only some boundaries of the cavity can be reserved for acoustical treatments. The acoustical material is not positioned anywhere but is rather patched at specified regions during the optimization process. In coping with this difficulty, noncontinuous design variables capable of fully describing the parameter of specified regions must therefore be introduced in addition to continuous ones. As a consequence of manipulating the problems associated with continuous and noncontinuous design variables, the SQP scheme is enhanced by a modified branch and bound method (BBM)[9–11] to effectively solve a general nonlinear passive noise control (PNC) optimization problem. Treating the PNC optimization in such a manner is the primary focus of this study, which is of essential concern for design engineers but has not yet been considered in a previous work.

An optimization problem is formed in this study which optimizes allocations of acoustical materials on the boundary in cavities by minimizing the objective function which is subjected to suitable constraints. Total acoustic potential energy of the control volume, similar to those in noise control problems, is selected here as the objective function. The optimization is performed in the frequency domain by assuming that the noise source is of harmonic excitation. Next, computer simulations of acoustical treatments in enclosures are performed and discussed for different arrangements. In those simulations, a two-dimensional cavity is used to verify the BEM-based optimization design tool. An irregularly shaped car cabin is then modeled for further studies.

I. BOUNDARY ELEMENT FORMULATION IN ACOUSTICS

Indirect BEM as derived by Chen and Schweikert[12] is a numerical technique that can be used to calculate the sound fields in a three-dimensional space. The method is a numerical implementation of Huygen's principle in acoustics. The optimal acoustical treatments on the boundary of the enclosures in this study are simulated from the response at field points of an acoustic system as illustrated in Fig. 1. Thus the derivation of optimal passive noise controllers can be formulated by using the indirect BEM technique. The numerical implementation of the indirect BEM technique in this study is customized from the general boundary element formulation. In summary, the process can be divided into the following steps.

Step 1: The nonhomogeneous Helmholtz equation, $\nabla^2 p + k^2 p = \psi_s(\mathbf{x}_s)$, is utilized in forming the problem, where p is the complex acoustic pressure and k is the wave number. The point noise source of strength ψ_s is located at $\mathbf{x}_s$.

Step 2: The general form of indirect BEM integral equations for pressure, velocity, and impedance (locally reacting) boundary conditions, respectively, are written as

$$p(\xi) = \int_B \sigma(b) p^*(b,\xi)\, dB + \int_D \psi_s(\mathbf{x}_s) p^*(\mathbf{x}_s,\xi)\, dD, \tag{1}$$

$$u(\xi) = c_b \sigma(\xi) + \int_b \sigma(b) u^*(b,\xi)\, dB + \int_D \psi_s(\mathbf{x}_s) u^*(\mathbf{x}_s,\xi)\, dD, \tag{2}$$

$$z(\xi) = p(\xi)/u(\xi), \tag{3}$$

where $\sigma(b)$ represents the fictitious source density function at the boundary point b, c_b is an integration constant as a result of the integral singularity,[13] and ξ is a dummy variable. The fundamental pressure solution p^* is the free space Green's function, $p^*(b,\xi) = 1/|b-\xi| e^{-jk|b-\xi|}$ and the fundamental velocity solution u^* can be related[14] to p^* by Euler's equation, $\rho\, \partial u/\partial t = -\nabla p$, where ρ is the density of air.

Step 3: A noncompatible, rectangular, linear element is selected to discretize the boundary of the acoustic system. Consequently, results can be obtained with reasonable computer capacity and time as a result of the need of optimization and model with a large number of elements. The volume integrals of ψ_s in Eqs. (1), (2), and (3) are then replaced by the summation term in light of the point noise sources. Hence, Eqs. (1), (2), and (3) are rewritten as

$$p(b_i) = \sum_{j=1}^{N_e} \int_{B_j} \sigma(b_j) p^*(b_j,b_i)\, dB_j + \sum_{l=1}^{N_s} \psi_{sl}(\mathbf{x}_{sl}) p^*(\mathbf{x}_{sl},b_i), \tag{4}$$

$$u(b_i) = c_b \sigma(b_i) + \sum_{j=1}^{N_e} \int_{B_j} \sigma(b_j) u^*(b_j,b_i)\, dB_j + \sum_{l=1}^{N_s} \psi_{sl}(\mathbf{x}_{sl}) u^*(\mathbf{x}_{sl},b_i), \tag{5}$$

$$0=\left(\sum_{j=1}^{N_e}\int_{B_j}\sigma(b_j)p^*(b_j,b_i)dB_j+\sum_{l=1}^{N_s}\psi_{sl}(\mathbf{x}_{sl})p^*(\mathbf{x}_{sl},b_i)\right)$$
$$-z(b_i)\left(c_b\sigma(b_i)+\sum_{j=1}^{N_e}\int_{B_j}\sigma(b_j)u^*(b_j,b_i)dB_j\right.$$
$$\left.+\sum_{l=1}^{N_s}\psi_{sl}(\mathbf{x}_{sl})u^*(\mathbf{x}_{sl},b_i)\right), \tag{6}$$

where N_e is the number of elements, N_s is the number of noise sources, B_j is the boundary contained by the jth element, and b_i is the ith node.

Step 4: A system of N_e equations for the N_e unknown σ's is obtained by writing Eqs. (4), (5), and/or (6) for each element according to the given boundary conditions. Thus a compact matrix form of Eq. (7) is solved for the fictitious source strength σ of each element:

$$\mathbf{A}\boldsymbol{\sigma}=\boldsymbol{\alpha}-\mathbf{B}\boldsymbol{\psi}_s, \tag{7}$$

where matrices **A** and **B** are computed from Eqs. (4), (5), and/or (6), and vector $\boldsymbol{\alpha}$ contains the values of boundary conditions. For instance, if element i has a pressure boundary condition, then

$$A_{ij}=\int_{B_j}p^*(b_j,b_i)dB_j, \tag{8}$$

$$B_{il}=p^*(\mathbf{x}_{sl},b_i), \tag{9}$$

$$\alpha_i=p(b_i). \tag{10}$$

Step 5: Finally, Eqs. (4) and (5) are used to find the acoustic pressure and particle velocity of the interior points, in which the boundary point b_i is replaced by the domain point x_i.

II. MATHEMATICAL MODEL FOR OPTIMIZATION PROBLEM

Generally, three elements are included in a well-defined mathematical statement of the constrained design optimization, i.e., design variables, objective function, and design constraints. The primary objective of this study is to form an optimization problem capable of optimizing placements of acoustical materials on the boundary of a cavity. Each element of optimization is described in the following.

A. Design variables

Assuming that the acoustical materials is only locally reacting, the normal impedance has the form $R(f)-jX(f)$, where R and X are the resistance and reactance parts, respectively, and are dependent on frequency f.[15] From a practical perspective, the candidates of design variables can be the number of pieces (n), centroid location (x,y,z), normal impedance (R,X), and size (A) of acoustical materials. The material-patched code (λ) of a boundary element can also be a design variable, where $\lambda=1$ or 0 implies that the element does or does not cover the acoustical materials. For brevity sake, the size of the acoustic materials is selected as the area of the boundary element, i.e., the size A is a constant. If the characteristic of the noise source is known and the sound field is only controlled by the acoustical materials, the acoustic pressure at field points of the cavity can be represented by

$$p_i=p_i(n,x,y,z,R,X,\lambda), \quad i=1,N_{\text{fp}}, \tag{11}$$

where N_{fp} is the total number of field points.

B. Objective function

Various objective functions have been used for the optimization of noise control, i.e., the total acoustic potential energy by Jo and Elliott,[16] weighted sum of the magnitudes of the squared pressures by Mollo and Bernhard,[17] average of acoustic pressures ratio by Tanaka *et al.*,[18] total acoustic power by Cunefare and Koopmann,[19] and space-average sound energy density by Yang *et al.*[20] All of these functions are deemed effective as a performance index, even though a slight difference occurs among them. The total acoustic potential energy of the control volume is, however, selected as the objective function in this study. Two control strategies, local and global,[21] can be applied where necessary. The objective function for various control strategies can always be formulated as

$$\Phi=\frac{1}{4\rho c^2}\int_V|p(n,x,y,z,R,X,\lambda)|^2\,dV, \tag{12}$$

where c and V are the speed of sound and the control volume, respectively. The Φ can only be measured by ideal distributed sensors, which may not be practical for application purposes. In practice, a reasonable number of acoustical pickups are uniformly positioned in the cavity to accumulate the response for formulating the discrete form of the objective function, as illustrated by Eq. (13):

$$\Psi=\frac{V}{4\rho c^2}\sum_{i=1}^{N_{\text{fp}}}|p_i(n,x,y,z,R,X,\lambda)|^2. \tag{13}$$

This form is implemented in the numerical simulations. The control volume V can notably be taken out of the summation only if the acoustical pickups are uniformly distributed throughout the cavity. Otherwise, the contribution of each pickups must be weighted.

C. Design constraints

All engineering systems are designed to perform within a given set of constraints which include limitations on resources, material failure, response of the system, and member sizes. Three types of constraints are introduced in this study, i.e., design bounds, equality constraints, and inequality constraints. Possible candidates for each type are defined in the following.

1. Design bounds

$$0\leq n\leq N_e, \tag{14}$$

$$x_l\leq x_i\leq x_u, \quad i=1,n, \tag{15}$$

$$y_l\leq y_i\leq y_u, \quad i=1,n, \tag{16}$$

$$z_l\leq z_i\leq z_u, \quad i=1,n, \tag{17}$$

$$R_l \leq R_i \leq R_u, \quad i=1,n, \tag{18}$$

$$X_l \leq X_i \leq X_u, \quad i=1,n, \tag{19}$$

$$\lambda_j \in \{0,1\}, \quad j=1,N_e, \tag{20}$$

where the subcripts l and u represent the lower and upper bound of the design variables, respectively.

2. Equality constraints

$$\lambda_1+\lambda_2+\cdots+\lambda_{N_e}=n. \tag{21}$$

This constraint implies that the sum of the patched codes must be equal to the number of pieces of acoustical materials utilized.

3. Inequality constraints

If the user wishes to maintain the specified sound pressure level (SPL) at particular locations, e.g., conforming to mandatory regulations, the following equation can be considered:

$$\text{SPL} \quad \text{at} \quad (x_j,y_j,z_j)-L_p \leq 0, \quad j=1,N_{\text{spl}}, \tag{22}$$

where L_p and N_{spl} are the specified SPL and number of selected locations, respectively.

D. Summary of optimization model

In summary, the design optimization model of this study finds the number of pieces (n), location (x,y,z), and impedance (R,X) of acoustical materials so as to minimize the total acoustic potential energy, which satisfies the required constraints. Generally, the aforementioned constrained optimization problem can be described mathematically while minimizing the objective function

$$f(\mathbf{x})=f(x_1,x_2,\ldots,x_N), \tag{23}$$

subject to the constraints

$$h_i(\mathbf{x})=0, \quad i=1,N_{\text{eql}}, \tag{24}$$

$$g_j(\mathbf{x}) \leq 0, \quad j=1,N_{\text{iql}}, \tag{25}$$

and the design bounds

$$\mathbf{x}_l \leq \mathbf{x} \leq \mathbf{x}_u, \tag{26}$$

where N_{eql} and N_{iql} are the number of equality and inequality constraints, respectively. It is a general mathematical model for the nonlinear single-objective constrained optimization problem. The optimum design $\mathbf{x}$ can be obtained by employing efficient minimization algorithms capable of solving the related subproblem for determining the search direction, as well as determining the step size by minimizing the descent function.[8]

E. Optimization algorithm

Multiple minima basically exist in the feasible domain of the preceding optimization problem along with a number of numerical nonlinear programming (NLP) methods which are capable of solving it. However, the sequential quadratic programming (SQP) is selected in this study because of its robustness and rapid convergence.[22–24] The SQP algorithm is a generalized gradient-descent optimization method and subsequently converges to a local rather than global optimum. This optimization method solves the quadratic programming subproblem to produce the direction of design improvement, and a step size along the search direction. The subproblem is obtained by using a quadratic approximation of the Lagrangian and linearizing the constraints as follows:

$$\min \nabla f(\mathbf{x}^k)^T \Delta\mathbf{x}^k+0.5\ \Delta\mathbf{x}^k\mathbf{H}^T \Delta\mathbf{x}^k, \tag{27}$$

subject to

$$h_i(\mathbf{x}^k)+\nabla h_i(\mathbf{x}^k)^T \Delta\mathbf{x}^k=0, \quad i=1,N_{\text{eql}}, \tag{28}$$

$$g_j(\mathbf{x}^k)+\nabla g_j(\mathbf{x}^k)^T \Delta\mathbf{x}^k \leq 0, \quad j=1,N_{\text{iql}}, \tag{29}$$

and

$$\mathbf{x}_l \leq \mathbf{x}^k+\Delta\mathbf{x}^k \leq \mathbf{x}_u, \tag{30}$$

where $\mathbf{H}$ is a positive definite approximation of the Hessian matrix, which is composed of the second partial derivatives of the Lagrangian function with respect to each of the design variables, and $\mathbf{x}^k$ is the current iterate. The Lagrangian function is formed here in terms of the objective function and constraints and is defined as $L(\mathbf{x},\boldsymbol{\mu})=f(\mathbf{x})+\Sigma\mu_i h_i(\mathbf{x})+\Sigma\mu_j g_j(\mathbf{x})$, where μ is the Lagrange multiplier. If $\Delta\mathbf{x}^k$ is selected as the solution of the subproblem, a line search can be utilized in finding the new point $\mathbf{x}^{k+1}$, i.e.,

$$\mathbf{x}^{k+1}=\mathbf{x}^k+\eta_k\ \Delta\mathbf{x}^k, \tag{31}$$

where the step size η_k is selected as 0.5^J with J as the smallest positive integer which satisfies a *descent function* having a lower value at the new point.[8] The descent function is basically formed by the objective function and maximum constraint violation[8] due to its simplicity and success in solving a large number of engineering design problems.[25,26] This iteration process is continued until the convergence test is passed; otherwise, the design variables are updated and the new iteration is executed.

To make use of well-established continuous optimization algorithms, most discrete optimization techniques are based on the assumption of transforming the noncontinuous solution space into multiple continuous solution sub-spaces. The optimization problems in each of these continuous subspaces are solved sequentially by imposing constraints on discreteness of the design variables. The optimal discrete solution is selected from among the continuous solutions obtained. The conventional discrete optimization techniques require too many executions of the continuous optimization scheme and, thus, is very time consuming.[9]

Here, an enhanced branch and bound method (BBM)[10,11] is employed to cope with the obstacles arising from noncontinuous design variables. In order to locate a discrete optimal solution using continuous optimization schemes, the BBM repeatedly delete portions of the original design space that do not contain allowable values of the noncontinuous design variables. This procedure is referred to as "branching." As illustrated in Fig. 2, the original design space is first divided into three sub-spaces with the allowable noncontinuous design values nearest the continuous optimal solution as the upper and lower bound of the left and right sub-spaces, re-

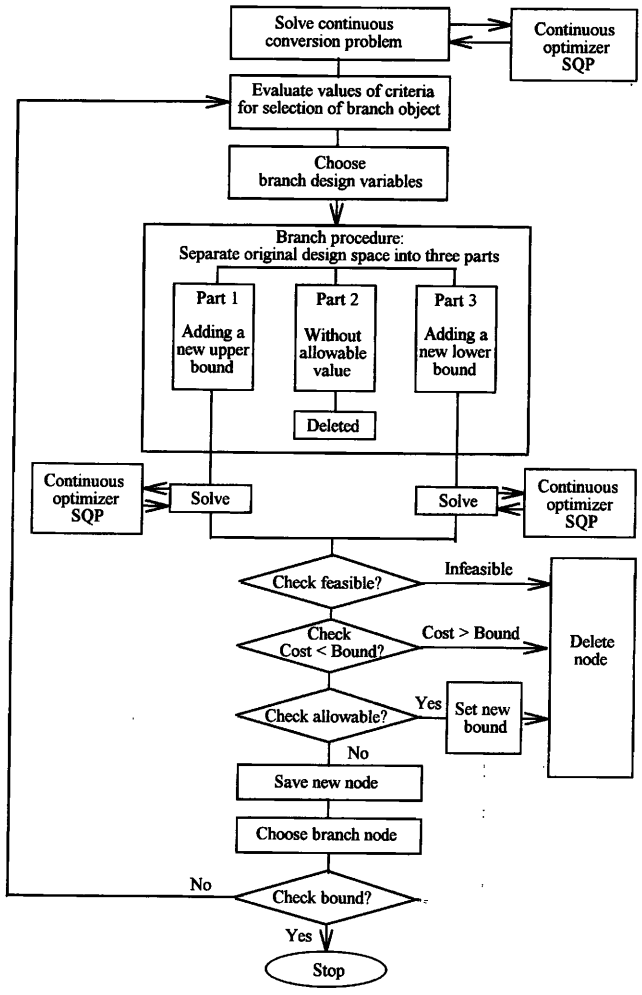

FIG. 2. Conceptual flow chart of the noncontinuous optimizer BBM.

spectively. The branching procedure must be repeated in each of the sub-spaces until a feasible optimal design is located. Each design sub-space is depicted as a "node" and a diagram of the branching is referred to as the "tree" of BBM. Theoretically, a discrete solution can be found if an exhaustive search of the tree is made.

If a feasible noncontinuous solution is obtained in the process of branching, the corresponding objective function value can be taken as a bound. Any other design sub-spaces that possess a continuous minimum cost larger than this bound need not be further branched since it would only generate higher cost values. This strategy is referred to as "bounding" and can be used to select a branching route intelligently, thereby avoiding complete and impartial searching through the tree.

Furthermore, all the procedures of the constrained optimization model defined in this study are incorporated into an architectural framework for the proposed design tool, as illustrated in Fig. 3. The communication between the BEM acoustical analysis and the BBM enhanced SQP optimization during the solution procedure is also shown in this architectural framework.

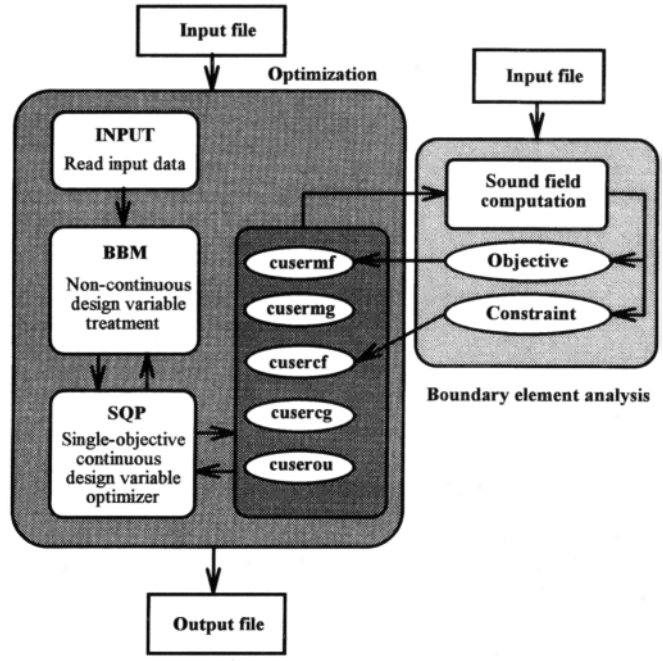

FIG. 3. Architectural framework of the proposed design tool, where **cuserxx** routines are user supplied functions. The **cusermf** and **cusermg** compute values of the objective and constraint functions, respectively. The **cusercf** and **cusercg** calculate gradients of the objective and constraint functions, respectively. However, the **cuserou** can provide additional data for verification.

III. COMPUTER SIMULATIONS

A. Verification of the BEM-based optimization algorithm

Numerical characteristics of the developed BEM-based optimization technique are investigated by conducting a computer simulation for design of acoustical treatments in a two-dimensional cavity (Fig. 4). The cavity with two openings has a dimension of $0.56\times0.32\times0.08$ m, i.e., slightly different from the one utilized by Bernhard and Takeo.[7] A point noise source of volume velocity 1 m^3/s is positioned at (0.14, 0, 0.04) and is a harmonic source at frequencies ranging between 1500 and 2000 Hz.

Two configurations of acoustical treatments, C1 and C2 (Fig. 4), are first simulated to make a qualitative comparison of the results with the concluding remarks in the previous work,[7] i.e., (1) it would appear that at a low frequency, where

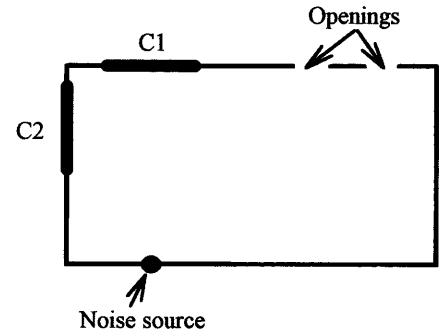

FIG. 4. Schematic diagram of a two-dimensional cavity utilized in Sec. III A.

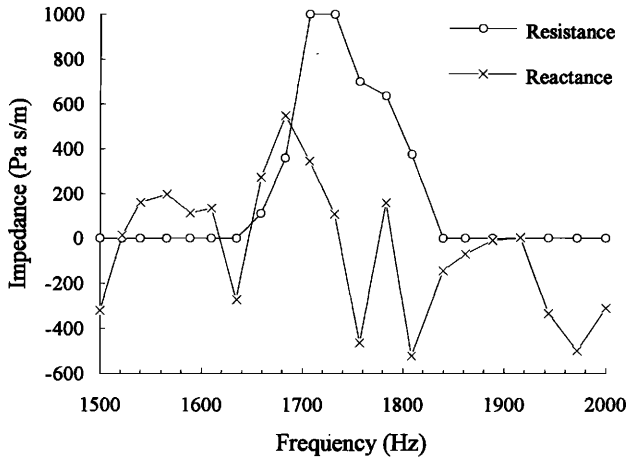

FIG. 5. Optimal acoustical treatments versus frequency at Cl configuration.

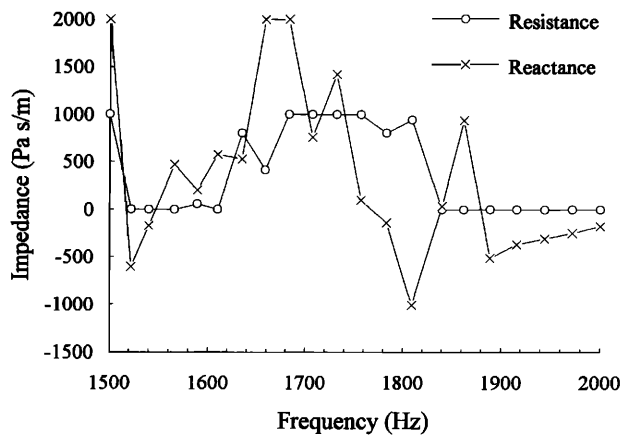

FIG. 7. Optimal acoustical treatments versus frequency at C2 configuration.

enclosures can properly be termed as tightly coupled, purely reactive noise control treatments are preferred; (2) there is also a particular optimal reactive impedance depending on the frequency, geometry, and design objective function. For illustrative purposes, the impedance (R,X) of acoustical materials is selected as the only design variable (i.e., acoustical material being fixed at specified location). The design bounds are set to $0 \leqslant R \leqslant 1000$ Pa s/m and $-2000 \leqslant X \leqslant 2000$ Pa s/m. No physical constraints are involved in this case. Consequently, acoustical impedance at *fixed* configuration (i.e., $n=1$) is optimized with the noise source of resonant or off-resonant excitation. Typical results are summarized in Figs. 5–8. The following general statements can be drawn from these numerical simulations.

(1) The optimal impedances of acoustical material vary with the exciting frequencies of the noise source and also change with locations of acoustical treatments. At resonances (i.e., 1540, 1610, and 1840 Hz in the frequency of interest) or near resonances, the optimal noise control treatments in this small cavity are more or less purely reactive (see Figs. 5 and 7) as a result of attenuation of the noise level by altering the mode shape. These remarks are quite similar to those concluded by Bernhard and Takeo.[7]

(2) In light of no obvious mode shape, however, the mechanism of controlling the noise level at off-resonances of the cavity can be different from that described at resonances. As also shown in Figs. 5 and 7, resistances (i.e., absorption) of the acoustical material are required in the off-resonant excitations for globally dissipating the acoustic energy in the control volume for better noise reduction.

(3) The objective function at resonances or near-resonances of the cavity decreases dramatically while the optimal impedances are obtained (Figs. 6 and 8). This can be considered as a consequence of a large reduction of SPL in the control volume. However, the objective function is insensitive to the variation of impedances of acoustical materials at off-resonances. Thus, the global minimum of this situation is difficult to be located. The local minimum can definitely be accepted from an engineering perspective if the improvement of design is obvious.

In summary, the major remarks of this simulation correlate sufficiently with those of Bernhard and Takeo.[7] Further studies of acoustical treatments in enclosures are thus supported by utilizing the proposed design tool of this work. Due to the powerfulness of the BBM enhanced SQP algorithm, the *location* and *impedance* of acoustical materials as design variables are simultaneously solved for the aforementioned case. Two more configurations, C3 and C4, are added to the current case for further investigations (Fig. 9). Additionally, design bounds of impedance are restricted to

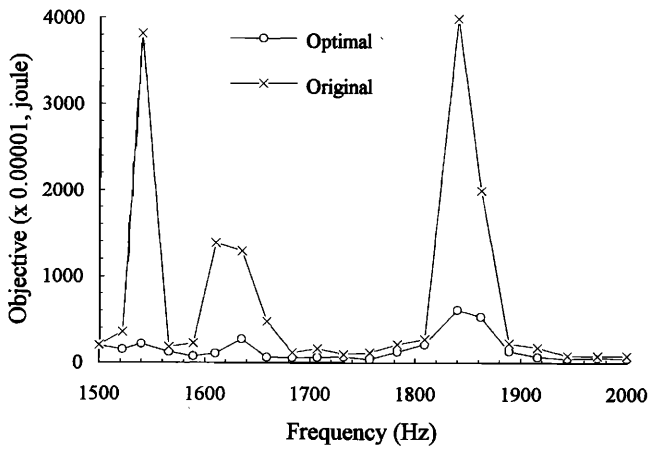

FIG. 6. Optimal objective function versus frequency at Cl configuration.

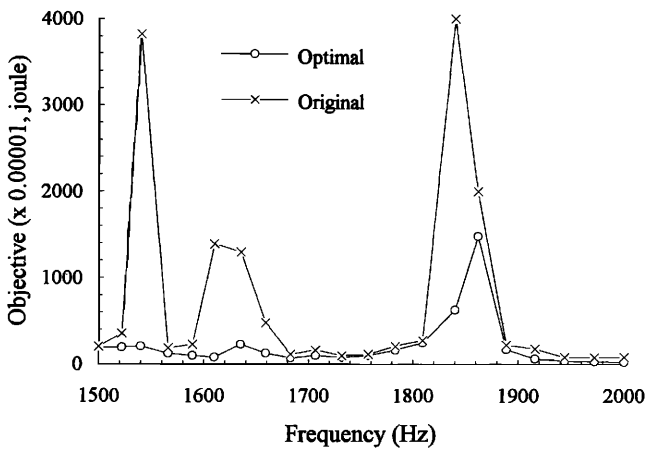

FIG. 8. Optimal objective function versus frequency at C2 configuration.

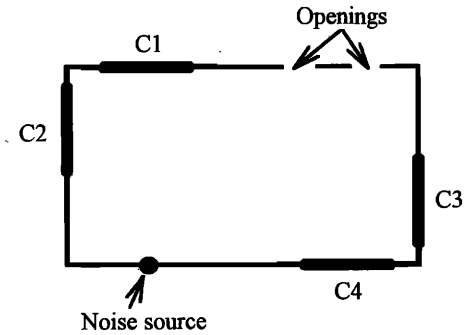

FIG. 9. Schematic diagram of a two-dimensional cavity utilized in Sec. III A.

$0 \leqslant R \leqslant 1000$ and $100 \leqslant X \leqslant 2000$ Pa s/m as a result of avoiding the possibility of zero impedance, which is approximated for a waterborne sound by the free surface of the ocean.[27] Here, only noise source of the resonance of the cavity is focused on, i.e., at frequencies of 1540, 1610, and 1840 Hz, in light of having a large acoustic potential energy. Three cases, i.e., patching the acoustical material at a single, two, and three configuration, are simulated, as indicated in Table I. As previously mentioned, optimal impedances for these cases are generally purely reactive. Also, optimal locations and impedances of acoustical treatments alter with the frequency of excitation. If the characteristic of the noise source is a narrow band with the specific resonance of a cavity, this information can be useful for better acoustical material patching in the preliminary design stage. Performance of using three pieces of acoustical material is deemed more generally effective than that of a single and double one, i.e., a 16% to 97% lower objective function. Table II indicates that the typical history of iterations while location and impedance of acoustical material are simultaneously considered as design variables.

B. Acoustical treatments in an irregularly shaped cavity

A car cabin of its dimensions shown in Fig. 10[28] is selected as a practical situation in which an irregularly shaped boundary occurs. The engine firing frequency dominates the internal noise level in a number of cars, particularly at higher engine speeds.[29] Therefore, control of engine-induced noise inside the car is of vital interest in this study. A frequency range of 20 to 200 Hz is focused upon as a result of the likelihood of a low-frequency, engine noise boom phenomenon which is increased by the current trend toward lighter car bodies and more powerful engines. The control volume utilized to compute the squared acoustic pressure (p^2) of the objective function is located in the vicinity of the driver's and passengers' heads in the cavity. For convenience, the seats in the cabin are removed, and rigid walls are assumed on the boundary unless otherwise stated. A noise source of volume velocity 1 m^3/s is positioned at (0.5, 0.14, 0.34) to simply simulate a single transmission path of the engine-induced noise. Five candidate regions are selected for patching acoustical materials, i.e., roof, floor, left door, right door, and back panels. Design bounds of impedance are $0 \leqslant R \leqslant 1000$ and $100 \leqslant X \leqslant 2000$ Pa s/m. SPL at passenger heads, i.e., locations of (2.3, 0.6, 1.2), (2.3, 1.4, 1.2), (3.2, 0.6, 1.2), and (3.2, 1.4, 1.2), must be smaller than 80 dB. This SPL value can be practically assigned if the characteristics of the noise source are precisely defined.

TABLE I. Optimal acoustical treatments in the resonant excitation of the two-dimensional cavity with $n=1$, 2, and 3, respectively.

n	Frequency Hz	Location C_i	Impedance Pa s/m (R,X)	Objective function $\times 10^{-3}$, joule	
				Original	Optimal
1	1540	C_2	(0, −119)	3821	208
	1610	C_1	(0, −100)	1388	116
	1840	C_1	(0, −180)	32441	6324
2	1540	C_2/C_4	(0, −429)	3821	171
	1610	C_1/C_3	(0, −294)	1388	91
	1840	C_2/C_4	(0, −183)	32441	217
3	1540	$C_1/C_2/C_4$	(0, −942)	3821	137
	1610	$C_1/C_3/C_4$	(0, −100)	1388	67
	1840	$C_2/C_3/C_4$	(0, −220)	32441	185

First, acoustical influences in the frequency range from 20 to 200 Hz at five regions are verified at specified impedance, as shown in Fig. 11. Acoustical influence is defined here as the average insertion loss (IL) in the frequency range of interest. However, the IL is known to be the difference of SPL in the control volume *with* and *without* the acoustical treatments. The *thickness of the shading* near the panel or *the number of the dB*, indicates the relative influence on the sound pressure reduction of the control volume *qualitatively* or *quantitatively*. This reduction is a result of patching acoustical material with *fixed* impedances to that particular panel across the frequency band of interest. This figure reveals that the major contributing panel to noise reduction is situated in the *floor* region. Of course, these results depend strongly upon the frequency range, control volume, characteristics of noise source, and specified impedance of acoustical material. However, computations such as these can provide useful information regarding contributing panels at frequencies characterizing important excitation of engine firing. From Fig. 11, acoustical influence of the floor panel (region) is obviously more dominant than others, i.e., a 6 to 7 dB higher IL.

In order to more fully comprehend the characteristics of acoustical treatments in the region of floor, a simulation of results shown in Figs. 12 and 13 is conducted. Again, the purely reactive impedance is preferred at the optimal acoustical treatments in this low frequency range. Reasons for this trend are similar to those mentioned in Sec. III A. However, a lower bound tendency of the optimal reactance can be related to the geometrical configuration of the cavity, position of noise source, and complexity of sound fields in the cabin. Furthermore, effectiveness of acoustical treatments is quite high at the resonant excitation of the car cabin due to a lower objective function (0.4%–6% of original one) and a higher insertion loss (13 dB on average).

Finally, acoustical treatments in the resonant excitation of the car cabin with location and impedance as design variables simultaneously are illustrated in Table III for $n=1$, 2

TABLE II. The typical history of iterations while using the location of the acoustical material as a design variable.

Acoustical treatments for a cavity of dimensions 0.56×0.32×0.08 m

The input data file in pnc. inp

NUMBER OF DESIGN VARIABLES =6
NUMBER OF OBJECTIVE FUNCTIONS =1
NUMBER OF EQUALITY CONSTRAINTS =1
NUMBER OF INEQUALITY CONSTRAINTS =0
MAXIMUM NUMBER OF ITERATIONS =100
INDEX OF PRINTING CODE =0
GRADIENT CALCULATION INDICATOR =1
NO. OF CONSECUTIVE ITER. FOR ACT =5
TOL. IN CONSTR. VIOL. AT OPT. =1.0000e−04
CONVERGENCE PARAMETER VALUE =1.0000e−04
DEL FOR F. D. GRAD. CALCULATION =1.0000e−01
ACCEPTABLE CHANGE IN COST FUNC. =1.0000e−09

::::: Type, Starting design and its limits ::::::

No.	Type	Design	Lower lim	Upper lim
1	Zero-one	0.0000e+00	0.0000e+00	1.0000e+00
2	Zero-one	1.0000e+00	0.0000e+00	1.0000e+00
3	Zero-one	0.0000e+00	0.0000e+00	1.0000e+00
4	Zero-one	1.0000e+00	0.0000e+00	1.0000e+00
5	Continue	0.0000e+00	0.0000e+00	1.0000e+03
6	Continue	1.0000e+02	1.0000e+02	2.0000e+03

First cycle:
Initial design:
X[1] 0.0000e+00 X[2] 1.0000e+00 X[3] 0.0000e+00 X[4] 1.0000e+00
X[5] 0.0000e+00 X[6] 1.0000e+02
*** Final design:: ***
*X[1] 0.0000e+00 *X[2] 5.0000e−01 *X[3] 1.0000e+00
*X[4] 5.0000e−01 *X[5] 0.0000e+00 *X[6] 1.9686e+02
*** Cost function at optimum=1.8992628e+02 ***
No. of calls for cost function evaluation (usermf) =700
No. of calls for cost function gradient evaluation (usermg) =0
No. of calls for constraint function evaluation (usercf) =700
No. of calls for constraint function gradients evaluation (usercg) =0
No. of total gradient evaluations =100

The following cycles are the BRANCH-AND-BOUND cycles:

Initial design:
X[1] 0.0000e+00 X[2] 1.0000e+00 X[3] 5.0000e−01 X[4] 0.0000e+00
X[5] 1.9686e+02
*** Final design:: ***
*X[1] 4.4432e−02 *X[2] 1.0000e+00 *X[3] 9.5557e−01
*X[4] 0.0000e+00 *X[5] 1.9318e+02
*** Cost function at optimum=2.3261524e+02 ***
No. of calls for cost function evaluation (usermf)=71
No. of calls for cost function gradient evaluation (usermg)=0
No. of calls for constraint function evaluation (usercf)=69
No. of calls for constraint function gradients evaluation (usercg)=0
No. of total gradient evaluations=6

TABLE II. (*Continued.*)

(The middle steps are deleted)

```
 Initial design:
  X[1] 0.0000e+00 X[2] 0.0000e+00 X[3] 0.0000e+00 X[4] 1.8345e+02
*** Final design:: ***
  *X[1] 0.0000e+00 *X[2] 0.0000e+00 *X[3] 0.0000e+00  *X[4] 1.8345e+02
*** Cost function at optimum=2.1746219e+02 ***
No. of calls for cost function evaluation (usermf)=30
No. of calls for cost function gradient evaluation (usermg)=0
No. of calls for constraint function evaluation (usercf)=29
No. of calls for constraint function gradients evaluation (usercf)=0
No. of calls gradient evaluations=2

Final results:
Number of iterations=1
Maximum constraint violation=0.00000e+00
Convergence parameter=1.48308e-01
The value of supercrition=2.17462e+02
The design variables:
  X[1] 0.0000e+00 X[2] 1.0000e+00 X[3] 0.0000e+00
  X[4] 1.0000e+00 X[5] 0.0000e+00 X[6] 1.8345e+02
Total number of calls of USERMF=2308
Total number of calls of USERMG=0
Total number of calls of USERCF=2304
Total number of calls of USERCG=0
No. of total eval. of grad=386
```

and 3, respectively. Some remarks can be drawn from these typical simulations.

(1) The optimal location of acoustical patching for the $n=1$ case is all of positioning in the *floor* region. Also, one of the optimal treatments for all of $n=2$ and 3 cases contains the *floor* panel. These results can directly correlate with the analysis of acoustical influence in the aforementioned section.

(2) In light of dominance of acoustical treatment in the floor region, performance of the $n=2$ and 3 cases does not have much of an improvement as compared with the $n=1$ case, except for the resonant excitations of 39 and 66 Hz.

(3) However, purely-reactive impedance preferred is not true for some particular situations. For instance, resistance is also required to optimally attenuate the noise at the excitations of 75 and 103 Hz for the $n=2$ case. This can be as a result of *either* the objective function being insensitive to the variation of impedance in the neighborhood of global minimum *or* other mechanisms which are not clearly known.

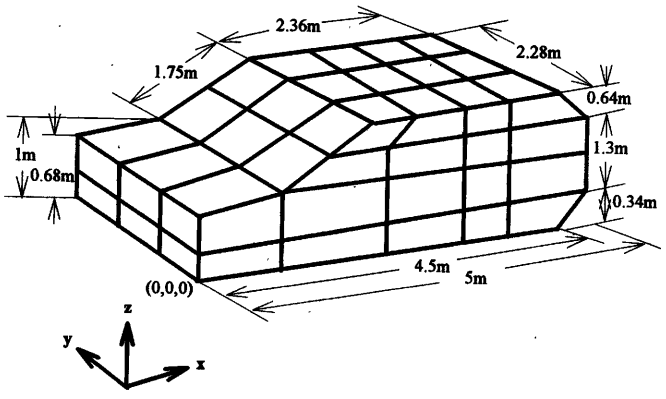

FIG. 10. The mesh and dimensions of a car cabin utilized in Sec. III B.

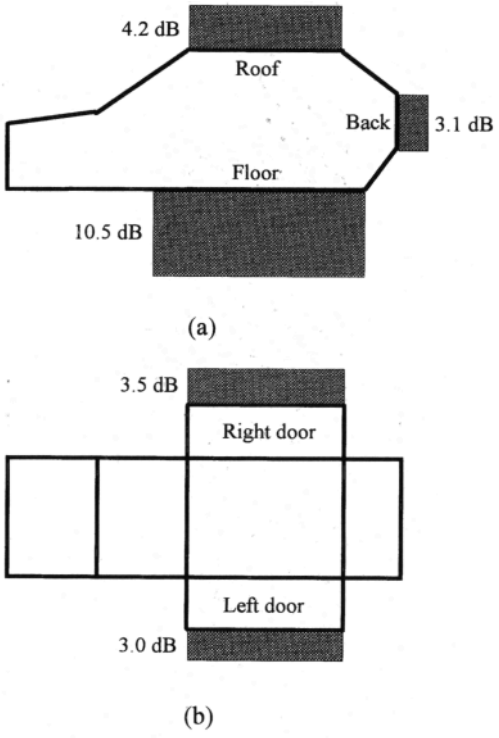

FIG. 11. Acoustical influence diagram: (a) side view, (b) top view.

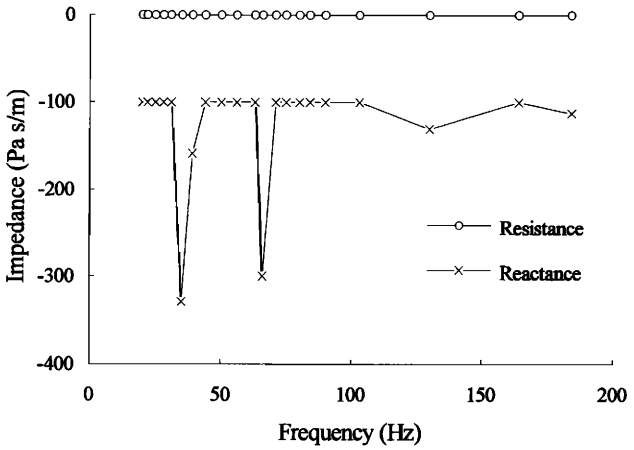

FIG. 12. Optimal impedance in the region of floor as a function of frequency for the car cabin.

(4) Performance for the $n=3$ case is not necessarily better than that for the $n=1$ and 2 cases as a result of complexities of primary sound fields in the cavity, dominance of acoustical treatment in the floor region, and local minimum searching of the algorithm. This knowledge implies that the number of piece of acoustical materials can be optimized if it is selected as a design variable.

IV. CONCLUSIONS

Combining the numerical BE acoustical analysis with the SQP optimization solver could be an effective tool for designing acoustical treatments in cavities at low frequency. The SQP optimization solver was enhanced in this study by the modified BBM procedure to simultaneously treat the practical applications of continuous and noncontinuous design variables. This would be especially useful while the conventional combinatorial design has become impractical. A small two-dimensional cavity was verified as well as the utility of the proposed design tool demonstrated by an irregularly shaped car cabin. Computer simulations indicated that at a low frequency, where enclosures can properly be termed as tightly coupled, purely reactive acoustical treatments are generally preferred at *resonances* or *near-resonances* of the two-dimensional cavity as well as at *the frequency of interest*

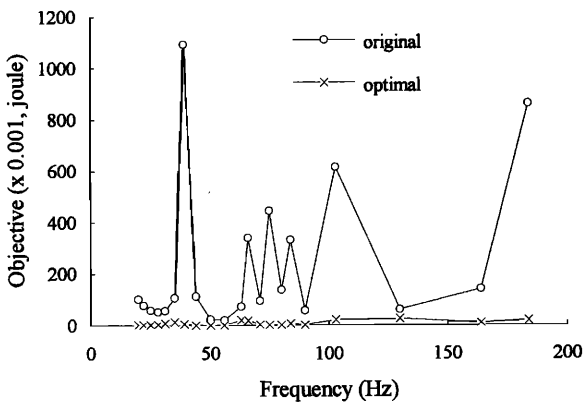

FIG. 13. Objective function in the region of floor as a function of frequency for the car cabin.

TABLE III. Optimal acoustical treatments in the resonant excitation of the car cabin with $n=1$, 2 and 3, where C, F, L, and R represent the regions of ceiling, floor, left, and right door panel, respectively.

n	Frequency Hz	Location	Impedance Pa s/m (R,X)	Objective function $\times 10^{-3}$, joule Original	Optimal	Insertion loss dB
	39	F	(0, −159)	1092	5	21
	66	F	(0, −300)	339	19	12
1	75	F	(0, −100)	445	3	23
	84	F	(0, −100)	332	7	14
	103	F	(0, −100)	616	22	15
	39	C/F	(0, −100)	1092	0.4	32
	66	C/F	(0, −100)	339	3	20
2	75	C/F	(240, −100)	445	2	24
	84	C/F	(0, −100)	332	5	18
	103	F/R	(272, −100)	616	7	19
	39	C/F/L	(0, −100)	1092	0.1	38
	66	F/L/R	(0, −100)	339	0.7	27
3	75	C/F/L	(0, −100)	445	9	18
	84	C/F/L	(0, −100)	332	5	18
	103	C/F/L	(0, −100)	616	19	15

in the car cabin. This general agreement between the present study and the previous work of Bernhard and Takeo[7] was considered adequate for the proposed tool to be utilized for the preliminary design study of acoustical treatments in enclosures. Furthermore, the optimal locations of acoustical treatments would always contain the region of dominant acoustical influence in the situation of multiple patching. However, capability of optimizing locations and impedances of acoustical material simultaneously were not considered in the previous work.

ACKNOWLEDGMENTS

The authors acknowledge the National Science Council, Taiwan, R.O.C. for partial support of this work under grant NSC 82-0401-E009-085. The Center for Measurement Standards of Industrial Technology Research Institute, Taiwan, R.O.C. is also appreciated for financially supporting T. C. Yang.

[1] D. Y. Maa, "Theory and Design of Microperoforated Panel Sound-Absorbing Constructions," Sci. Sinica **18**, 55–71 (1975).
[2] D. Y. Maa, "Microperoforated Panel Wideband Absorbers," Noise Control Eng. J. **29** (3), 77–84 (1987).
[3] J. Lee and G. W. Swenson, Jr., "Compact Sound Absorbers for Low Frequencies," Noise Control Eng. J. **38** (3), 109–117 (1992).
[4] R. S. Jackson, "The Performance of Acoustic Hoods at Low Frequencies," Acustica **12**, 139–152 (1962).
[5] M. C. Junger, "Sound Transmission Through an Elastic Enclosure Acoustically Closely Coupled to a Noise Source," ASME Paper No. 70-WA/DE-12 (1970).
[6] L. W. Tweed and D. R. Tree, "Three Methods for Predicting the Insertion Loss of Close-Fitting Acoustical Enclosures," Noise Control Eng. **10** (2), 74–79 (1978).
[7] R. J. Bernhard and S. Takeo, "A Finite Element Procedure for Design of Cavity Acoustical Treatments," J. Acoust. Soc. Am. **83**, 2224–2230 (1988).
[8] J. S. Arora, *Introduction to Optimum Design* (McGraw-Hill, New York, 1989).
[9] C. H. Tseng, L. W. Wang, and S. F. Ling, "Numerical Study of Branch-and-Bound Method in Structural Optimization," Technical Report AODL-

90-02, National Chiao Tung University, Taiwan, ROC (1990).
[10] C. H. Tseng, L. W. Wang, and S. F. Ling, "Enhancing the Branch-and-Bound Structural Optimization," Proc. Int. Conf. Comput. Methods Eng., Singapore, 1180–1185 (1992).
[11] C. H. Tseng, L. W. Wang, and S. F. Ling, "Enhancing the Branch-and-Bound Method for Structural Optimization," to appear in the ASCE J. Struct. Eng. (1995).
[12] L. H. Chen and D. G. Schweikert, "Sound Radiation from an Arbitrary Body," J. Acoust. Soc. Am. **35**, 1626–1632 (1963).
[13] R. D. Ciskowski and C. A. Brebbia, *Boundary Element Methods in Acoustics* (Elsevier Applied Science, London, 1991).
[14] L. E. Kinsler, A. R. Frey, A. B. Coppens, and J. V. Sanders, *Fundamentals of Acoustics*. (Wiley, New York, 1982).
[15] A. Craggs, "A Finite Element Method for Modeling Dissipative Mufflers with a Locally Reactive Lining," J. Sound Vib. **54** (2), 285–296 (1977).
[16] C. H. Jo and S. J. Elliott, "Active Control of Low Frequency Sound Transmission Between Rooms," J. Acoust. Soc. Am. **92**, 1461–1472 (1992).
[17] C. G. Mollo and R. J. Bernhard, "Generalized Method of Predicting Optimal Performance of Active Noise Controllers," AIAA J. **27** (11), 1473–1478 (1989).
[18] M. Tanaka, Y. Yamada, and M. Shirotori, "Boundary Element Method Applied to Simulation of Active Noise Control in Ducts," JSME Int. J. **35** (3), 387–392 (1992).
[19] K. A. Cunefare and G. H. Koopmann, "A Boundary Element Approach to Optimization of Active Noise Control Sources on Three-Dimensional Structures," ASME J. Vib. Acoust. **113**, 387–394 (1991).
[20] T. C. Yang, C. H. Tseng, and C. H. Huang, "An Interface Coupler for Finite Element Analysis and Optimization," Proc. Sixteenth National Conf. Theoretical and Applied Mechanics, Keelung, Taiwan, ROC, 887–894 (1992).
[21] T. C. Yang, C. H. Tseng and S. F. Ling, "Constrained Optimization of Active Noise Control Systems in Enclosures," J. Acoust. Soc. Am. **95**, 3390–3399 (1994).
[22] C. H. Tseng and J. S. Arora, "On Implementation of Computational Algorithms for Optimal Design, Part I: Preliminary Investigation," Int. J. Num. Methods Eng. **26**, 1365–1384 (1988).
[23] C. H. Tseng and J. S. Arora, "On Implementation of Computational Algorithms for Optimal Design, part II: Extensive Numerical Investigation," Int. J. Num. Methods Eng. **26**, 1385–1402 (1988).
[24] C. H. Tseng and W. C. Liao, "Integrated Software for Multifunctional Optimization," Tech. Report AODL-90-01, Dept. of Mechanical Eng., National Chiao Tung Univ., Taiwan, ROC (1990).
[25] B. N. Pshenichny, "Algorithms for the General Problem of Mathematical Programming," Kibernetica, No. 5 (1978).
[26] A. D. Belegundu and J. S. Arora, "A Recursive Quadratic Programming Algorithm with Active Set Strategy for Optimal Design," Int. J. Num. Methods Eng. **20**, 803–816 (1984).
[27] M. C. Junger and D. Feit, *Sound, Structures, and Their Interaction* (MIT, Cambridge, 1986).
[28] M. R. Bai, "Study of Acoustic Resonance in Enclosures Using Eigenanalysis Based on Boundary Element Methods," J. Acoust. Soc. Am. **91**, 2529–2538 (1992).
[29] P. A. Nelson and S. J. Elliott, *Active Noise Control of Sound* (Academic, London, 1992).